

# Scale Setting with Gradient Flow on (2+1)-flavor HISQ ensembles

Johannes H. Weber (they/them)  
w. R.N. Larsen, S. Mukherjee, P. Petreczky, H.-T. Shu

[Larsen:2025wvg]

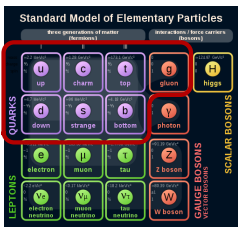
[Technische Universität Darmstadt]



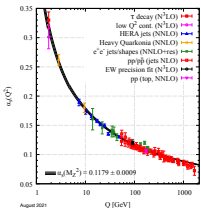
Scale setting: Precision lattice QCD for particle and nuclear physics,  
ECT\*, Trento, Italy, 03/03/2025

# QCD in the standard model

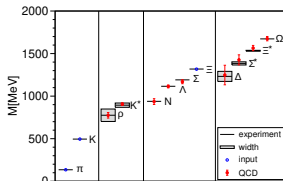
- **Standard Model of Particle Physics:** most elementary, **precisely tested** theory of nature; inconsistencies would provide hints of **New Physics**.
- **Nuclear matter** (quarks, gluons): **Quantum Chromodynamics (QCD)**.
- **Flavors:** *u, d, s:* **light**; *c:* **intermediate**; *b:* **heavy**; *t:* (irrelevant in QCD).



QCD running coupling



Light hadron spectrum



[BMW, Science 322, 2008]

- **Confinement:** neither quarks nor gluons are observable, but only **hadrons**.
- Non-perturbative QCD with **fully-controlled systematics** ⇒ **lattice QCD**.

## Physical vs theory scales

- No explicit lattice scale, **determine**  $a(g^2, \dots)$  in scale setting.
- **Good: Cheap, precise, simple.** ✓
- **Bad: Cutoff,  $N_f$ , mass, volume dependence. Non-QCD effects.** ✗

## Physical vs theory scales

- No explicit lattice scale, **determine**  $a(g^2, \dots)$  in scale setting.
- **Good: Cheap, precise, simple.** ✓
- **Bad: Cutoff,  $N_f$ , mass, volume dependence. Non-QCD effects.** ✗

### Absolute scale setting with physical scales

- **Absolute scale setting:** LQCD observable  $\leftrightarrow$  real world physical scale.
- **Quark mass dependence or non-QCD effects** are relevant.
- **Low precision** of LQCD observables and real-world data may be an issue.

## Physical vs theory scales

- No explicit lattice scale, **determine**  $a(g^2, \dots)$  in scale setting.
- **Good: Cheap, precise, simple.** ✓
- **Bad: Cutoff,  $N_f$ , mass, volume dependence. Non-QCD effects.** ✗

### Absolute scale setting with physical scales

- **Absolute scale setting:** LQCD observable  $\leftrightarrow$  **real world physical scale.**
- **Quark mass dependence or non-QCD effects** are relevant.
- **Low precision** of LQCD observables and real-world data may be an issue.

### Relative scale setting with theory scales

- **Relative scale setting:** LQCD observable  $\leftrightarrow$  **another LQCD observable.**
- **Quark mass dependence or non-QCD effects** are largely irrelevant.
- **High precision** of certain LQCD observables is easy to achieve.

## Two different types of physical scales

### Decay constants (isospin limit)

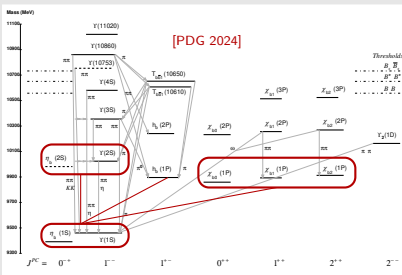
$\eta_s$ ✓	$af_{\eta_s}^{\text{meas}} = af_0 + 2sam_s^{\text{input}}$	$= 128.34(85) \text{ MeV}$	[Davies:2009tsa].
<b>Kaon</b> ✓	$af_K^{\text{meas}} = af_0 + s(am_l^{\text{input}} + am_s^{\text{input}})$	$= 110.10(64) \text{ MeV}$	[HotQCD:2014kol].
<b>P4S</b> ✓	$af_{p4s}^{\text{meas}} = af_0 + 2sa(0.4 m_s^{\text{input}})$	$= 108.89(49) \text{ MeV}$	[MILC:2012znn].
<b>Pion</b> ✗	$af_{\pi}^{\text{meas}} = af_0 + 2sam_l^{\text{input}}$	$= 92.28(14) \text{ MeV}$	[FLAG:2024oxs].

# Two different types of physical scales

## Decay constants (isospin limit)

$\eta_s$ ✓	$af_{\eta_s}^{\text{meas}} = af_0 + 2sam_s^{\text{input}}$	$= 128.34(85) \text{ MeV}$	[Davies:2009tsa].
<b>Kaon</b> ✓	$af_K^{\text{meas}} = af_0 + s(am_l^{\text{input}} + am_s^{\text{input}})$	$= 110.10(64) \text{ MeV}$	[HotQCD:2014kol].
<b>P4S</b> ✓	$af_{p4s}^{\text{meas}} = af_0 + 2sa(0.4 m_s^{\text{input}})$	$= 108.89(49) \text{ MeV}$	[MILC:2012znn].
<b>Pion</b> ✗	$af_{\pi}^{\text{meas}} = af_0 + 2sam_l^{\text{input}}$	$= 92.28(14) \text{ MeV}$	[FLAG:2024oxs].

## Bottomonia splittings



- Use **spin averages in S, P-waves**:  
 $M_S = (M_{\eta} + 3M_{\Upsilon})/4$ ,  
 $M_{\chi_b} = (M_{\chi_{b0}} + 3M_{\chi_{b1}} + 5M_{\chi_{b2}})/9$ .
- Differences  $\Delta M_X = M_X - M_S(1S)$ .
- Splittings from [PDG 2024].  
 $\Delta M_{\eta_b} = 454.5(0.9) \text{ MeV}$ .  
 $\Delta M_{\chi_b} = 455.0(0.6) \text{ MeV}$ .  
 $\Delta M_S(2S) = 584.5(2.3) \text{ MeV}$ .
- Bottom mass  $\Rightarrow$  **cutoff effects** ✗

## Two different types of theory scales

### Gradient flow scales

$$\sqrt{t_i} \quad c_i = \tau_F^2 \langle E(\tau_F) \rangle |_{\tau_F=t_i} \quad c_{0,2} = 0.3, 0.2 \quad [\text{Luscher:2010iy}].$$

$$w_i \quad c_i = \tau_F \frac{d}{d\tau_F} [\tau_F^2 \langle E(\tau_F) \rangle] |_{\tau_F=w_i^2} \quad c_{0,2} = 0.3, 0.2 \quad [\text{BMW:2012hcm}].$$

- For **coarse** lattices:  $t_1$ ,  $\sqrt{w_1}$  with  $c_1 = 0.7$  introduced earlier [Borsanyi:2023wno].
- For **fine** lattices:  $t_2$ ,  $\sqrt{w_2}$  with  $c_2 = 0.2$  introduced recently [Larsen:2025wvg].
- Gradient flow time  $\tau_F$ : **smooth, arb. small increments, no cubic SB** ✓.



## Two different types of theory scales

### Gradient flow scales

$$\sqrt{t_i} \quad c_i = \tau_F^2 \langle E(\tau_F) \rangle |_{\tau_F=t_i} \quad c_{0,2} = 0.3, 0.2 \quad [\text{Luscher:2010iy}].$$

$$w_i \quad c_i = \tau_F \frac{d}{d\tau_F} [\tau_F^2 \langle E(\tau_F) \rangle] |_{\tau_F=w_i^2} \quad c_{0,2} = 0.3, 0.2 \quad [\text{BMW:2012hcm}].$$

- For **coarse** lattices:  $t_1$ ,  $\sqrt{w_1}$  with  $c_1 = 0.7$  introduced earlier [Borsanyi:2023wno].
- For **fine** lattices:  $t_2$ ,  $\sqrt{w_2}$  with  $c_2 = 0.2$  introduced recently [Larsen:2025wvg].
- Gradient flow time  $\tau_F$ : **smooth, arb. small increments, no cubic SB** ✓.

### Potential scales

- Static  $Q\bar{Q}$  4D-correlator via Wilson loops or gauge-fixed Wilson line corr.

$$r_i \quad c_i = (r/a)^2 \frac{d}{d(r/a)} [\langle aE_0(r/a) \rangle] |_{r=r_i} \quad c_{1,2} = 1.0, 0.5 \quad [\text{Sommer:1993ce}].$$

- For **coarse** lattices:  $r_0$  with  $c_0 = 1.65$  [Sommer:1993ce].
- For **most** lattices:  $r_1$  with  $c_1 = 1.00$  [Bernard:2000gd].
- For **fine** lattices:  $r_2$  with  $c_2 = 0.50$  [Bazavov:2017dsy].
- Static  $Q\bar{Q}$  separation  $r$ : **non-smooth, discrete,  $O(3)$  to cubic SB** ✗.

## (2+1)-flavor HISQ ensembles

- **HotQCD ensembles**,  $\frac{m_l}{m_s} = \frac{1}{20}$  or  $\frac{1}{5}$  [HotQCD:2014kol], [Bazavov:2017dsy], [Altenkort:2023oms].
- Generated with **MILC** or **SIMULATEQCD** codes [MILC], [HotQCD:2023ghu].
- **Tree-level improved Lüscher-Weisz action** [Luscher:1984xn], [Luscher:1985zq].
- **(2 + 1) flavors with HISQ action** [Follana:2006rc].
- Almost **physical light quarks**:  $M_\pi = 161$  or  $322$  MeV, respectively.
- **Physical strange quarks**: unmixed  $M_{\eta_s} = 695$  MeV instead of 685.8 MeV.

$\beta$	$am_s$	$am_l$	$N_\sigma$	$N_\tau$	# conf.
7.030	0.0356	0.00178	48	48	900
7.150	0.0320	0.00160	48	64	395
7.280	0.0280	0.00142	48	64	398
7.373	0.0250	0.00125	48	64	554
7.596	0.0202	0.00101	64	64	577
7.825	0.0164	0.0082	64	64	471
8.000	0.01299	0.002598	64	64	1004
8.200	0.01071	0.002142	64	64	961
8.249	0.01011	0.002022	64	64	2241
8.400	0.00887	0.001774	64	64	2372

# Overview

- 1 Introduction
  - Scales
  - (2+1)-flavor HISQ ensembles
- 2 Gradient flow
  - Improved flow
  - Flow scale ratios
  - Ratios with potential scales
- 3 Physical results
  - Leptonic decay constants
  - Bottomonia splittings
  - Comparison à la FLAG
- 4 Weak coupling
  - $\Lambda_{\overline{MS}}$  from gradient flow coupling
- 5 Summary

# Formalism

- **Gradient flow** is a continuous, analytic smearing [Narayanan:2006rf], [Luscher:2009eq],

$$B_\mu(x, \tau_F = 0) = A_\mu(x), \quad \partial_{\tau_F} B_\mu(x, \tau_F) = D_\nu G_{\nu\mu}.$$

$$V(x, \mu)|_{\tau_F=0} = U(x, \mu), \quad \partial_{\tau_F} V(x, \mu, \tau_F) = -g_0^2 \{ \partial_{x,\mu} S_G(V) \} V(x, \mu, \tau_F).$$

- Realizes a **diffusive process** at tree level [Luscher:2010iy],

$$B_\mu(x, \tau_F) = \int d^4y K_{\tau_F}(x-y) A_\mu(y), \quad K_{\tau_F}(z) = \int \frac{d^4p}{(2\pi)^4} e^{ipz} e^{-\tau_F p^2} = \frac{e^{-z^2/4\tau_F}}{(4\pi\tau_F)^2}.$$

suppresses UV fluctuations: **reduces noise**, achieves renormalization.

- **Zeuthen flow** ( $\mathcal{O}(a^2)$ -improved evolution) for  $\{ \partial_{x,\mu} S_G(V) \}$ : [Ramos:2015baa].

# Formalism

- **Gradient flow** is a continuous, analytic smearing [Narayanan:2006rf], [Luscher:2009eq],

$$B_\mu(x, \tau_F = 0) = A_\mu(x), \quad \partial\tau_F B_\mu(x, \tau_F) = D_\nu G_{\nu\mu}.$$

$$V(x, \mu)|_{\tau_F=0} = U(x, \mu), \quad \partial\tau_F V(x, \mu, \tau_F) = -g_0^2 \{ \partial_{x,\mu} S_G(V) \} V(x, \mu, \tau_F).$$

- Realizes a **diffusive process** at tree level [Luscher:2010iy],

$$B_\mu(x, \tau_F) = \int d^4y K_{\tau_F}(x-y) A_\mu(y), \quad K_{\tau_F}(z) = \int \frac{d^4p}{(2\pi)^4} e^{ipz} e^{-\tau_F p^2} = \frac{e^{-z^2/4\tau_F}}{(4\pi\tau_F)^2}.$$

suppresses UV fluctuations: **reduces noise**, achieves renormalization.

- **Zeuthen flow** ( $\mathcal{O}(a^2)$ -improved evolution) for  $\{ \partial_{x,\mu} S_G(V) \}$ : [Ramos:2015baa].

- **Action density** as observable (four-volume averaged),

$$E(\tau_F, x) = -\frac{1}{2} \text{Tr} \{ F_{\mu\nu}(x, \tau_F) F_{\mu\nu}(x, \tau_F) \}.$$

- **Field strength** with clover or **improved discretizations** [Bilson-Thompson:2002xlt],

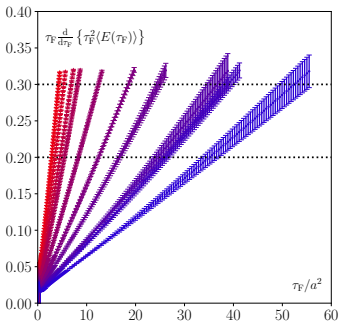
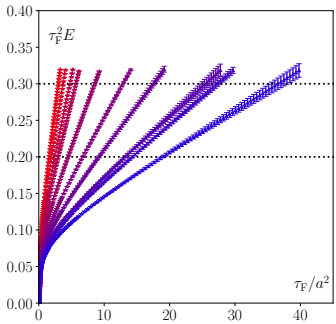
$$\hat{F}_{\mu\nu}^{\text{clo}}(n) = -\frac{i}{8} (Q_{\mu\nu}(n) - Q_{\nu\mu}(n)) \equiv C_{\mu\nu}^{(1,1)}(n),$$

$$\hat{F}_{\mu\nu}^{\text{imp}}(n) = \frac{5}{3} C_{\mu\nu}^{(1,1)}(n) - \frac{1}{3} C_{\mu\nu}^{(1,2)}(n).$$

$Q_{\mu\nu}(n)$ : sum of  $\mu, \nu$  plaquettes around site  $n$ ;  $C_{\mu\nu}^{(a,b)}(n)$  is generalization.

## Improved flow

$\beta$	7.03	7.15	7.28	7.373	7.596	7.825	8.000	8.200	8.249	8.400
$\frac{\sqrt{t_0}}{a}$ (c)	1.8259(5)	2.0217(8)	2.2636(13)	2.4549(19)	2.9847(28)	3.634(9)	4.228(33)	5.083(79)	5.262(50)	6.076(108)
$\frac{\sqrt{t_0}}{a}$ (i)	1.7298(5)	1.9334(7)	2.1831(13)	2.3799(19)	2.9218(30)	3.586(7)	4.184(33)	5.044(78)	5.225(50)	6.045(106)
$\frac{\sqrt{t_2}}{a}$ (c)	1.3891(2)	1.5276(4)	1.6076(5)	1.8320(7)	2.2048(12)	2.669(3)	3.096(12)	3.688(21)	3.837(26)	4.399(32)
$\frac{\sqrt{t_2}}{a}$ (i)	1.2593(2)	1.4056(3)	1.5841(4)	1.7244(7)	2.1116(12)	2.591(3)	3.027(11)	3.629(20)	3.780(25)	4.347(29)
$\frac{w_0}{a}$ (c)	2.0730(13)	2.3159(21)	2.6203(36)	2.8575(48)	3.5194(73)	4.292(24)	4.978(83)	6.156(345)	6.233(81)	7.293(330)
$\frac{w_0}{a}$ (i)	2.0674(13)	2.3121(22)	2.6178(37)	2.8558(50)	3.5193(72)	4.304(19)	4.978(83)	6.156(345)	6.233(81)	7.297(333)
$\frac{w_2}{a}$ (c)	1.6832(8)	1.8826(13)	2.1302(15)	2.3258(27)	2.8653(40)	3.510(13)	4.083(47)	4.999(188)	5.109(60)	5.954(199)
$\frac{w_2}{a}$ (i)	1.6883(8)	1.8893(14)	2.1380(16)	2.3341(27)	2.8740(44)	3.524(11)	4.089(47)	5.006(189)	5.115(60)	5.962(201)



- $\beta$
- 7.030
  - 7.150
  - 7.280
  - 7.373
  - 7.596
  - 7.825
  - 8.000
  - 8.200
  - 8.249
  - 8.400

## Beta function and scale ratios

## Beta function (Allton fits)

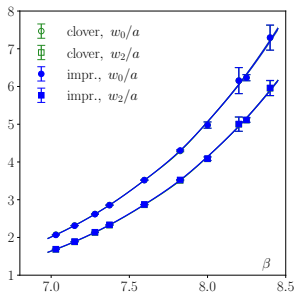
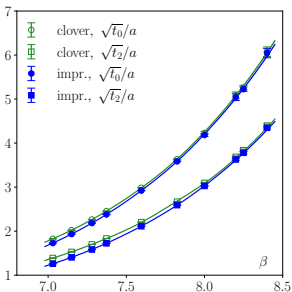
## ■ Beta function with Allton-type Ansatz

[Allton:1996dn],

$$\ln\left(\frac{\sqrt{t_i}}{a}\right) = \frac{1 + d_{2i}\left(\frac{10}{\beta}\right) f^2(\beta)}{c_{0i} f(\beta) + c_{2i}\left(\frac{10}{\beta}\right) f^3(\beta)}, \quad \ln\left(\frac{w_i}{a}\right) = \frac{1 + d'_{2i}\left(\frac{10}{\beta}\right) f^2(\beta)}{c'_{0i} f(\beta) + c'_{2i}\left(\frac{10}{\beta}\right) f^3(\beta)},$$

$$f(\beta) = \left(\frac{10b_0}{\beta}\right)^{-\frac{b_1}{2b_0^2}} \exp\left(-\frac{\beta}{20b_0}\right), \quad \beta = \frac{10}{g_0^2}, \quad b_0 = \frac{9}{(4\pi)^2}, \quad b_1 = \frac{1}{(4\pi^4)} \quad @ \quad N_f = 3.$$

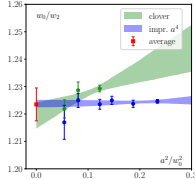
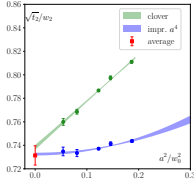
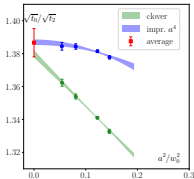
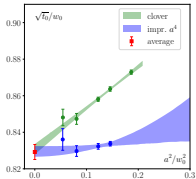
- Two different LCPs due to  $m_l$ : include extra factor  $(1 + c_{mi}(am_s + 2am_l))$ .
- Allton fits at red.  $\chi^2 = 0.8 \dots 1.9$ , except  $\frac{\sqrt{t_2}}{a}$  (clov) at red.  $\chi^2 = 15.5$ .



## Flow scale ratios

## Scale ratios

- $\frac{m_l}{m_s} = \frac{1}{20}$  ensembles: **ratios of flow scales**  $\frac{\sqrt{t_0}}{w_0}$ ,  $\frac{\sqrt{t_2}}{w_2}$ ,  $\frac{\sqrt{t_0}}{\sqrt{t_2}}$ ,  $\frac{w_0}{w_2}$ , via clov./imp.
- **Binning/bootstrapping determined by larger auto-correlation time.**
- Clov. as  $a^2$ , imp. as  $\alpha_s a^2$ ,  $a^2$ ,  $a^4$  via 3...6 betas, red.  $\chi^2 \simeq 0.3 \dots 1.9$ .

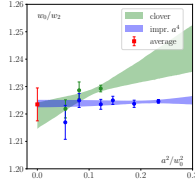
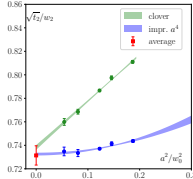
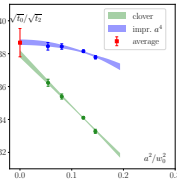
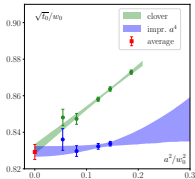




## Flow scale ratios

## Scale ratios

- $\frac{m_l}{m_s} = \frac{1}{20}$  ensembles: **ratios of flow scales**  $\frac{\sqrt{t_0}}{w_0}$ ,  $\frac{\sqrt{t_2}}{w_2}$ ,  $\frac{\sqrt{t_0}}{\sqrt{t_2}}$ ,  $\frac{w_0}{w_2}$ , via clov./imp.
- **Binning/bootstrapping determined by larger auto-correlation time.**
- Clov. as  $a^2$ , imp. as  $\alpha_s a^2$ ,  $a^2$ ,  $a^4$  via 3...6 betas, red.  $\chi^2 \simeq 0.3 \dots 1.9$ .



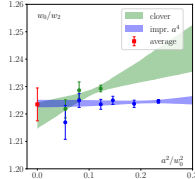
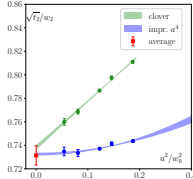
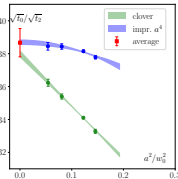
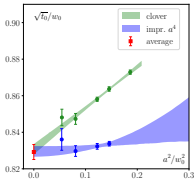
- Stat. error from wgt. mean of best fits (red.  $\chi^2 \simeq 1.0$ ) of each form.
- Syst. error due to max deviation from weighted mean, symmetrized.

$$\frac{\sqrt{t_0}}{w_0} = 0.8292(26)(15), \quad \frac{\sqrt{t_0}}{\sqrt{t_2}} = 1.3867(18)(68), \quad \frac{\sqrt{t_2}}{w_2} = 0.7314(15)(67), \quad \frac{w_0}{w_2} = 1.2235(19)(41).$$

## Flow scale ratios

## Scale ratios

- $\frac{m_l}{m_s} = \frac{1}{20}$  ensembles: ratios of flow scales  $\frac{\sqrt{t_0}}{w_0}$ ,  $\frac{\sqrt{t_2}}{w_2}$ ,  $\frac{\sqrt{t_0}}{\sqrt{t_2}}$ ,  $\frac{w_0}{w_2}$ , via clov./imp.
- Binning/bootstrapping determined by larger auto-correlation time.
- Clov. as  $a^2$ , imp. as  $\alpha_s a^2$ ,  $a^2$ ,  $a^4$  via 3...6 betas, red.  $\chi^2 \simeq 0.3 \dots 1.9$ .



- Stat. error from wgt. mean of best fits (red.  $\chi^2 \simeq 1.0$ ) of each form.
- Syst. error due to max deviation from weighted mean, symmetrized.

$$\frac{\sqrt{t_0}}{w_0} = 0.8292(26)(15), \quad \frac{\sqrt{t_0}}{\sqrt{t_2}} = 1.3867(18)(68), \quad \frac{\sqrt{t_2}}{w_2} = 0.7314(15)(67), \quad \frac{w_0}{w_2} = 1.2235(19)(41).$$

- Consistent w.  $N_f = 2 + 1 + 1$  estimates of ETM or HPQCD Collaborations:

$$\frac{\sqrt{t_0}}{w_0} = 0.82930(65)$$

[Extended Twisted Mass : 2021qui],

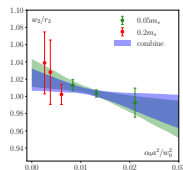
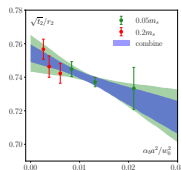
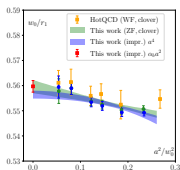
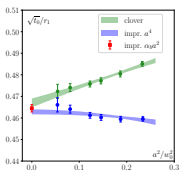
$$\frac{\sqrt{t_0}}{w_0} = 0.835(8)$$

[Dowdall : 2013rya].

## Ratios with potential scales

## Ratios with potential scales

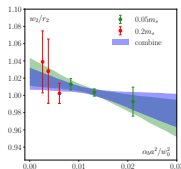
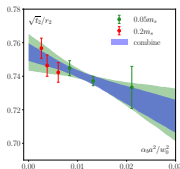
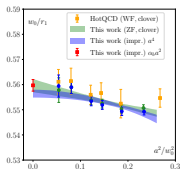
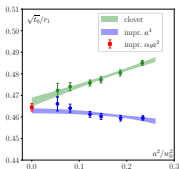
- $\frac{m_l}{m_s} = \frac{1}{20}$  ensembles: **ratios**  $\frac{\sqrt{t_0}}{r_1}, \frac{w_0}{r_1}$ , via clov./imp.
- $\frac{m_l}{m_s} = \frac{1}{20}$  combined w.  $\frac{m_l}{m_s} = \frac{1}{5}$  ensembles: **ratios**  $\frac{\sqrt{t_2}}{r_2}, \frac{w_2}{r_2}$ , via imp..



## Ratios with potential scales

## Ratios with potential scales

- $\frac{m_l}{m_s} = \frac{1}{20}$  ensembles: **ratios**  $\frac{\sqrt{t_0}}{r_1}, \frac{w_0}{r_1}$ , via clov./imp.
- $\frac{m_l}{m_s} = \frac{1}{20}$  combined w.  $\frac{m_l}{m_s} = \frac{1}{5}$  ensembles: **ratios**  $\frac{\sqrt{t_2}}{r_2}, \frac{w_2}{r_2}$ , via imp..

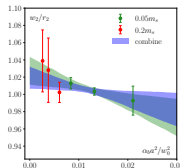
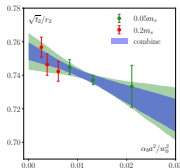
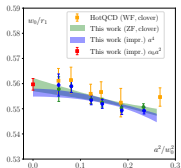
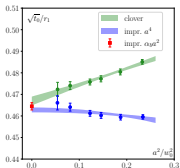


$$\frac{r_1}{\sqrt{t_0}} = 2.1530(78), \quad \frac{r_1}{w_0} = 1.7866(74), \quad \frac{\sqrt{t_2}}{r_2} = 0.7544(52), \quad \frac{w_2}{r_2} = 1.0265(142).$$

## Ratios with potential scales

## Ratios with potential scales

- $\frac{m_l}{m_s} = \frac{1}{20}$  ensembles: **ratios**  $\frac{\sqrt{t_0}}{r_1}, \frac{w_0}{r_1}$ , via clov./imp.
- $\frac{m_l}{m_s} = \frac{1}{20}$  combined w.  $\frac{m_l}{m_s} = \frac{1}{5}$  ensembles: **ratios**  $\frac{\sqrt{t_2}}{r_2}, \frac{w_2}{r_2}$ , via imp..



$$\frac{r_1}{\sqrt{t_0}} = 2.1530(78), \quad \frac{r_1}{w_0} = 1.7866(74), \quad \frac{\sqrt{t_2}}{r_2} = 0.7544(52), \quad \frac{w_2}{r_2} = 1.0265(142).$$

■ **Consistent** w. HotQCD, HPQCD, or combined TUMQCD & MILC:

- $\frac{r_1}{w_0} = 1.7797(67)$       ©  $N_f=2+1$  [HotQCD : 2014kol],
- $\frac{r_1}{w_0} = 1.789(26)$       ©  $N_f=2+1+1$  [Dowdall : 2013rya],
- $\frac{r_1}{\sqrt{t_0}} = 2.1601(83)$       ©  $N_f=2+1+1$  [MILC : 2015tqx],
- $\frac{r_1}{w_0} = 1.7749(96)$       ©  $N_f=2+1+1$  [Brambilla : 2022het].

## Extrapolation to physical point

- Pseudoscalar decay constants from **conserved axial current** with HISQ.
- Avoid via **strange quarks** much **taste-breaking or noise** (due to light  $q$ ).

## Extrapolation to physical point

- Pseudoscalar decay constants from **conserved axial current** with HISQ.
- Avoid via **strange quarks** much **taste-breaking** or **noise** (due to light  $q$ ).
- **Extrapolate** from  $M_{\eta_s}^{\text{LCP}} = 695 \text{ MeV}$  to  $M_{\eta_s}^{\text{phys}} = 685.8 \text{ MeV}$ , and  $\frac{m_l}{m_s} = \frac{1}{27.3}$ ,

$$af_{\eta_s}^{\text{phys}}(\beta) = af_{\eta_s}^{\text{meas}}(\beta) + 2s \cdot \left[ am_s^{\text{LCP}}(\beta) \left( \frac{m_{\eta_s}^{\text{phys}}}{m_{\eta_s}^{\text{LCP}}} \right)^2 - am_s^{\text{input}}(\beta) \right],$$

$$af_K^{\text{phys}}(\beta) = af_K^{\text{meas}}(\beta) + s \cdot \left[ am_s^{\text{LCP}}(\beta) \left( \frac{m_{\eta_s}^{\text{phys}}}{m_{\eta_s}^{\text{LCP}}} \right)^2 \cdot \frac{28.3}{27.3} - am_s^{\text{input}}(\beta) \cdot \frac{21}{20} \right].$$

- LCP strange quark mass at each beta via [HotQCD:2014kol]

$$\frac{r_1}{a} \cdot am_s^{\text{LCP}} = \frac{r_1}{a} \cdot am^{\text{RGI}} \left( \frac{20b_0}{\beta} \right)^{4/9} \frac{1+m_1 \frac{10}{\beta} f^2(\beta) + m_2 \left( \frac{10}{\beta} \right)^2 f^2(\beta) + m_3 \frac{10}{\beta} f^4(\beta)}{1+dm_1 \frac{10}{\beta} f^2(\beta)}$$

- $\frac{r_1}{a}, am^{\text{RGI}}, m_1, m_2, m_3, dm_1$ , prop. errors of  $\frac{r_1}{a}, am^{\text{RGI}}$  via **Gaussian bootstrap**.

## Extrapolation to physical point

- Pseudoscalar decay constants from **conserved axial current** with HISQ.
- Avoid via **strange quarks** much **taste-breaking** or **noise** (due to light  $q$ ).
- **Extrapolate** from  $M_{\eta_s}^{\text{LCP}} = 695$  MeV to  $M_{\eta_s}^{\text{phys}} = 685.8$  MeV, and  $\frac{m_l}{m_s} = \frac{1}{27.3}$ ,

$$af_{\eta_s}^{\text{phys}}(\beta) = af_{\eta_s}^{\text{meas}}(\beta) + 2s \cdot \left[ am_s^{\text{LCP}}(\beta) \left( \frac{m_{\eta_s}^{\text{phys}}}{m_{\eta_s}^{\text{LCP}}} \right)^2 - am_s^{\text{input}}(\beta) \right],$$

$$af_K^{\text{phys}}(\beta) = af_K^{\text{meas}}(\beta) + s \cdot \left[ am_s^{\text{LCP}}(\beta) \left( \frac{m_{\eta_s}^{\text{phys}}}{m_{\eta_s}^{\text{LCP}}} \right)^2 \cdot \frac{28.3}{27.3} - am_s^{\text{input}}(\beta) \cdot \frac{21}{20} \right].$$

- LCP strange quark mass at each beta via [HotQCD:2014kol]

$$\frac{r_1}{a} \cdot am_s^{\text{LCP}} = \frac{r_1}{a} \cdot am^{\text{RGI}} \left( \frac{20b_0}{\beta} \right)^{4/9} \frac{1+m_1 \frac{10}{\beta} f^2(\beta) + m_2 \left( \frac{10}{\beta} \right)^2 f^2(\beta) + m_3 \frac{10}{\beta} f^4(\beta)}{1+dm_1 \frac{10}{\beta} f^2(\beta)}$$

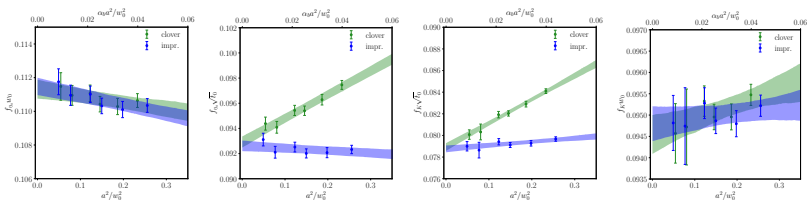
- $\frac{r_1}{a}, am^{\text{RGI}}, m_1, m_2, m_3, dm_1$ , prop. errors of  $\frac{r_1}{a}, am^{\text{RGI}}$  via **Gaussian bootstrap**.
- Assume **theory scales**  $\frac{\sqrt{t_0}}{a}, \frac{w_0}{a}, \frac{r_1}{a}$  are **independent of LCP/mistuning**.



## Flow scales from decay constants

## Scale ratios

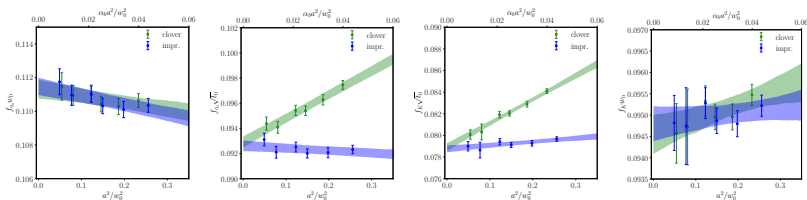
- $\frac{m_l}{m_s} = \frac{1}{20}$  ensembles: products  $w_0 f_{\eta_s}, \sqrt{t_0} f_{\eta_s}, \sqrt{t_0} f_K, w_0 f_K$ , via clov./imp.
- **Mixed bootstrap** due to extrapolation of  $f_{K,\eta_s}$  to physical point.
- $a^2$  for clov.,  $\alpha_s a^2$  or  $a^4$  for imp.; via 6 betas, red.  $\chi^2 \simeq 0.9 \dots 1.1$ .



## Flow scales from decay constants

## Scale ratios

- $\frac{m_l}{m_s} = \frac{1}{20}$  ensembles: products  $w_0 f_{\eta_s}, \sqrt{t_0} f_{\eta_s}, \sqrt{t_0} f_K, w_0 f_K$ , via clov./imp.
- **Mixed bootstrap** due to extrapolation of  $f_{K,\eta_s}$  to physical point.
- $a^2$  for clov.,  $\alpha_s a^2$  or  $a^4$  for imp.; via 6 betas, red.  $\chi^2 \simeq 0.9 \dots 1.1$ .



- All extrapolations agree, quoting  $\alpha_s a^2$  and imp.:

	$f_{\eta_s}^{\text{meas}} w_0$	$f_{\eta_s}^{\text{meas}} \sqrt{t_0}$	$f_K^{\text{meas}} \sqrt{t_0}$	$f_K^{\text{meas}} w_0$	$\frac{r_1}{\sqrt{t_0}}$	$\frac{r_1}{w_0}$
clov	0.11132(56)	0.09292(44)	0.07893(36)	0.09455(45)	2.1530(78)	1.7866(74)
impr.	0.11148(52)	0.09261(42)	0.07876(32)	0.09480(41)	2.1506(86)	1.7835(80)

$$\sqrt{t_0} = 0.14239(65)(94) \text{ fm},$$

$$\sqrt{t_0} = 0.14133(57)(82) \text{ fm},$$

$$w_0 = 0.17139(80)(113) \text{ fm},$$

$$w_0 = 0.17012(74)(98) \text{ fm},$$

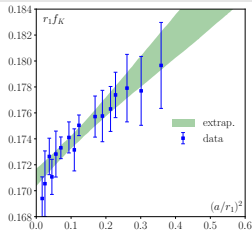
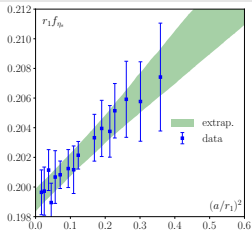
via  $f_{\eta_s}$ ,

via  $f_K$ .

# Potential scales from decay constants

## Potential scales from decay constants

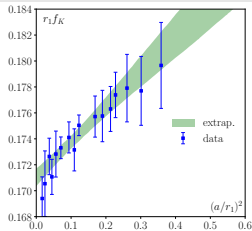
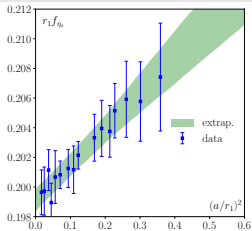
- Products of  $r_1$  with  $\sqrt{t_0}$ ,  $w_0$ ,  $f_{\eta_s}$ ,  $f_K$ .
- Continuum extrapolation of  $r_1 f_{K,\eta_s}$  with **more, coarser lattices** [HotQCD:2014kol].



# Potential scales from decay constants

## Potential scales from decay constants

- Products of  $r_1$  with  $\sqrt{t_0}$ ,  $w_0$ ,  $f_{\eta_s}$ ,  $f_K$ .
- Continuum extrapolation of  $r_1 f_{K,\eta_s}$  with **more, coarser lattices** [HotQCD:2014kol].

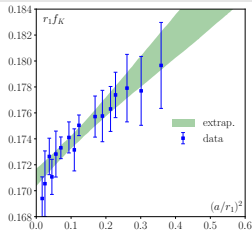
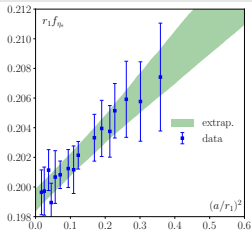


	$\sqrt{t_0}$	$w_0$	$f_{\eta_s}$	$f_K$
$r_1$	0.3053(37) fm	0.3050(38) fm	0.3062(23) fm	0.3065(22) fm

# Potential scales from decay constants

## Potential scales from decay constants

- Products of  $r_1$  with  $\sqrt{t_0}$ ,  $w_0$ ,  $f_{\eta_s}$ ,  $f_K$ .
- Continuum extrapolation of  $r_1 f_{K,\eta_s}$  with **more, coarser lattices** [HotQCD:2014kol].



	$\sqrt{t_0}$	$w_0$	$f_{\eta_s}$	$f_K$
$r_1$	0.3053(37) fm	0.3050(38) fm	0.3062(23) fm	0.3065(22) fm

- **Consistent w. TUMQCD, lower than MILC, RBC, or HPQCD:**

$$r_1 = 0.3037(26) \text{ fm}$$

$$r_1 = 0.3106(8)(14)(4) \text{ fm}$$

$$r_1 = 0.3209(26) \text{ fm}$$

$$r_1 = 0.333(9) \text{ fm}$$

$$\textcircled{c} N_f=2+1+1 \quad [\text{Brambilla} : 2022\text{het}] ,$$

$$\textcircled{c} N_f=2+1 \quad [\text{MILC} : 2010\text{hzw}] ,$$

$$\textcircled{c} N_f=2+1 \quad [\text{RBC} : 2010\text{qam}] ,$$

$$\textcircled{c} N_f=2+1+1 \quad [\text{Dowdall} : 2013\text{rya}] .$$

# Lattice NRQCD

- **Bottomonia splittings** for scale setting [Gray:2005ur], [Davies:2009tsa], [HPQCD:2011qwj].
- **Heavy quarks via  $\mathcal{O}(v^6)$ -improved lattice NRQCD** [Meinel:2009rd], [Meinel:2010pv].
- **Bottomonia levels computed on HotQCD ensembles** [Larsen:2019zqv], [Ding:2025fvo].

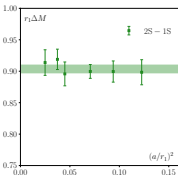
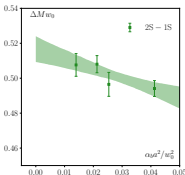
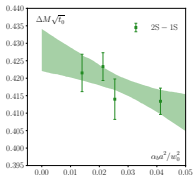
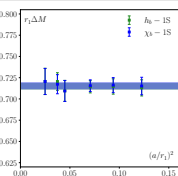
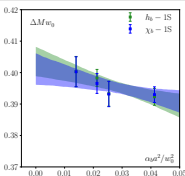
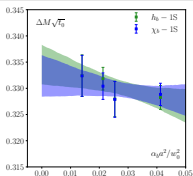
state	$\Delta M$ [MeV]	$\Delta M(PDG)$ [MeV]
$\Upsilon(3S)$	906.0(25.0)(5.2)	910.3(0.7)
$h_b(2P)$	804.4(35.8)(4.7)	814.9(1.3)
$\chi_{b2}(2P)$	809.2(36.2)(4.7)	823.8(0.9)
$\chi_{b1}(2P)$	802.2(34.9)(4.7)	810.6(0.7)
$\chi_{b0}(2P)$	786.8(32.7)(4.6)	787.6(0.8)
$\Upsilon(2S)$	582.7(9.8)(3.4)	578.4(0.6)
$h_b(1P)$	454.5(4.7)(2.6)	454.4(0.9)
$\chi_{b2}(1P)$	463.3(4.8)(2.7)	467.3(0.6)
$\chi_{b1}(1P)$	448.9(4.6)(2.6)	447.9(0.6)
$\chi_{b0}(1P)$	421.3(4.7)(2.4)	414.5(0.7)
hyperfine(3S)	13.4(6.2)(0.1)	NA
hyperfine(2S)	24.1(1.0)(0.1)	24.5(4.5)

- **Lattice NRQCD levels deviate from PDG by 0.2-1.2% .**

## Scales from bottomonia splittings

## Ratios with potential scales

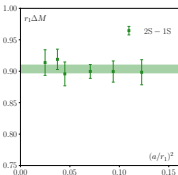
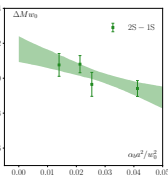
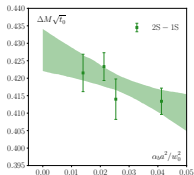
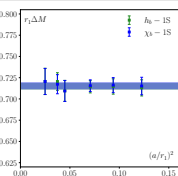
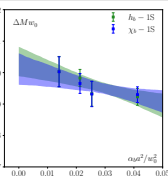
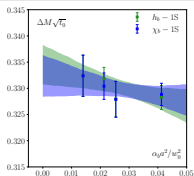
- $\frac{m_l}{m_s} = \frac{1}{20}$  ensembles: extrapolate **products** of  $\Delta M_X$  with  $\sqrt{t_0}, w_0, r_1$  **via imp.?**
- Due to lattice NRQCD levels **estimate 1% systematic error** on  $\Delta M_X$ .



## Scales from bottomonia splittings

## Ratios with potential scales

- $\frac{m_l}{m_s} = \frac{1}{20}$  ensembles: extrapolate **products** of  $\Delta M_X$  with  $\sqrt{t_0}, w_0, r_1$  **via imp.?**
- Due to lattice NRQCD levels **estimate 1% systematic error** on  $\Delta M_X$ .



	$\Delta M\sqrt{t_0}$	$\Delta Mw_0$	$\Delta Mr_1$	$\sqrt{t_0}$ [fm]	$w_0$ [fm]	$r_1$ [fm]
$h_b - 1S$	0.3330(53)	0.4024(63)	0.7150 (41)	0.1453(17)(15)	0.1752(21)(18)	0.3105(18)(31)
$\chi_b - 1S$	0.3325(52)	0.4018(62)	0.7155(42)	0.1441(17)(14)	0.1739(21)(17)	0.3104(18)(31)
2S - 1S	0.4243(76)	0.5128(91)	0.9036(70)	0.1477(40)(15)	0.1783(49)(18)	0.3119(76)(31)

Systematically higher than  $\sqrt{t_0}, w_0, r_1$  from decay constants, agrees w. MILC.



## Comparison à la FLAG

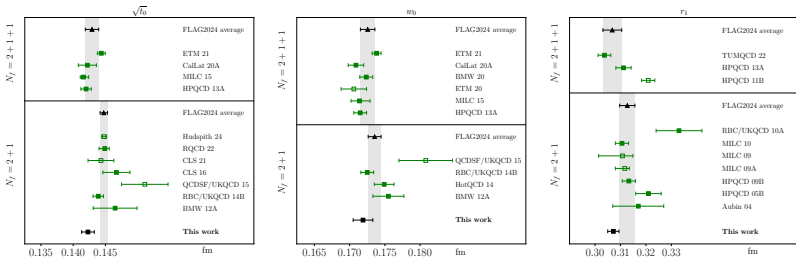
- Choice of the physical scale matters at one sigma level!

	$\sqrt{t_0}$ [fm]	$w_0$ [fm]	$r_1$ [fm]
$f_{\eta_s}$	0.14239(65)(94)	0.17139(80)(113)	0.3062(23)
$f_K$	0.14133(57)(82)	0.17012(74)(98)	0.3065(22)
$h_b - 1S$	0.1453(17)(15)	0.1752(21)(18)	0.3105(18)(31)
$\chi_b - 1S$	0.1441(17)(14)	0.1739(21)(17)	0.3104(18)(31)
$2S - 1S$	0.1477(40)(15)	0.1783(49)(18)	0.3119(76)(31)
wgt. avg.	0.14229 (98)	0.17190 (140)	0.3072 (22)

# Comparison à la FLAG

- Choice of the physical scale matters at one sigma level!

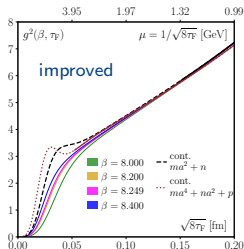
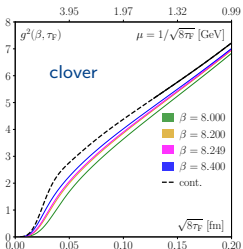
	$\sqrt{t_0}$ [fm]	$w_0$ [fm]	$r_1$ [fm]
$f_{\eta_s}$	0.14239(65)(94)	0.17139(80)(113)	0.3062(23)
$f_K$	0.14133(57)(82)	0.17012(74)(98)	0.3065(22)
$h_b - 1S$	0.1453(17)(15)	0.1752(21)(18)	0.3105(18)(31)
$\chi_b - 1S$	0.1441(17)(14)	0.1739(21)(17)	0.3104(18)(31)
$2S - 1S$	0.1477(40)(15)	0.1783(49)(18)	0.3119(76)(31)
wgt. avg.	0.14229 (98)	0.17190 (140)	0.3072 (22)



- $N_f = 2 + 1$  or  $N_f = 2 + 1 + 1$  results are consistent due to decoupling.
- Our  $N_f = 2 + 1$  results are lower than FLAG averages.
- No obvious link between staggered ensembles and values of scales.

## Gradient flow coupling

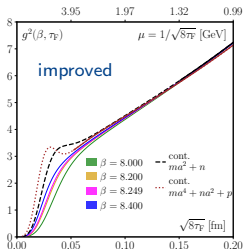
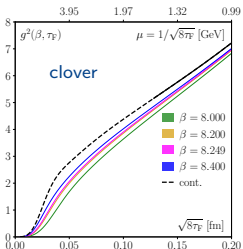
- Define **gradient flow coupling**  $g_{\text{flow}}^2 = \frac{128\pi^2\tau_F^2}{3(N_c^2-1)} \langle E \rangle$  [Fodor:2012td], [Hasenfratz:2019hpg], associated with a flow scale  $\mu_{\text{flow}} \simeq \sqrt{\frac{1}{\tau_F}}$  (usually  $\frac{1}{\sqrt{8\tau_F}}$ ).



- Solid lines: extrapolations w. red.  $\chi^2 < 1.5$ . Focus on imp/quartic.

## Gradient flow coupling

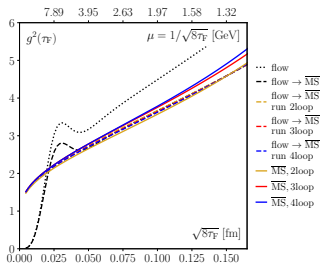
- Define **gradient flow coupling**  $g_{\text{flow}}^2 = \frac{128\pi^2\tau_F^2}{3(N_c^2-1)} \langle E \rangle$  [Fodor:2012td], [Hasenfratz:2019hpg], associated with a flow scale  $\mu_{\text{flow}} \simeq \sqrt{\frac{1}{\tau_F}}$  (usually  $\frac{1}{\sqrt{8\tau_F}}$ ).



- Solid lines: extrapolations w. red.  $\chi^2 < 1.5$ . Focus on imp/quartic.
- Scheme change** from gradient flow to  $\overline{\text{MS}}$  known at NNLO [Harlander:2021esn]

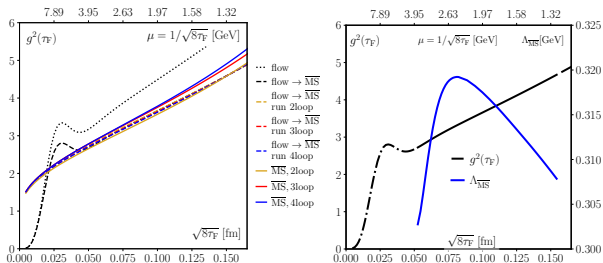
$$\alpha_{\text{flow}} = \alpha_{\overline{\text{MS}}} \left( 1 + k_1 \alpha_{\overline{\text{MS}}} + k_2 \alpha_{\overline{\text{MS}}}^2 \right) \quad \text{for} \quad \mu_{\overline{\text{MS}}}^2 = \mu_{\text{flow}}^2, \\ k_1 = 1.098 + 0.008 N_f, \quad k_2 = -0.982 - 0.070 N_f + 0.002 N_f^2.$$

# Lambda extraction



- To control both **continuum extrapolation** and **scheme conversion** choose a **reference point** above  $\mu_{\text{flow}} \geq 1.278 \text{ GeV}$  (i.e.  $\sqrt{8\tau_F} \leq 0.1543 \text{ fm}$ ).
- $g_{\text{flow}}^2$  from gradient flow to  $\overline{\text{MS}}$ , ran up from ref. point  $\mu_{\text{flow}} \geq 1.278 \text{ GeV}$  vs  $g_{\overline{\text{MS}}}^2$  ran down from  $g_{\overline{\text{MS}}}^2 = 0$  using  $\Lambda_{\overline{\text{MS}}} = 338 \text{ MeV}$ , at different loop orders.

# Lambda extraction



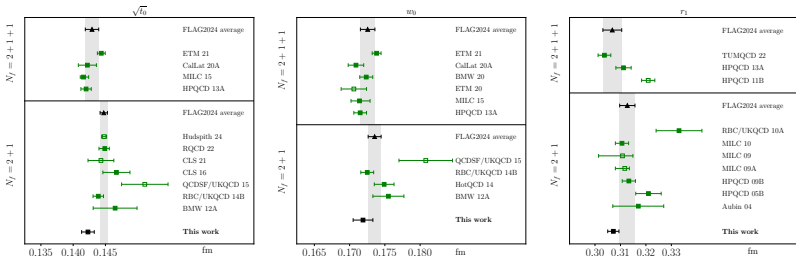
- To control both **continuum extrapolation** and **scheme conversion** choose a **reference point** above  $\mu_{\text{flow}} \geq 1.278 \text{ GeV}$  (i.e.  $\sqrt{8\tau_F} \leq 0.1543 \text{ fm}$ ).
- $g_{\text{flow}}^2$  from gradient flow to  $\overline{\text{MS}}$ , ran up from ref. point  $\mu_{\text{flow}} \geq 1.278 \text{ GeV}$  vs  $g_{\overline{\text{MS}}}^2$  ran down from  $g_{\overline{\text{MS}}}^2 = 0$  using  $\Lambda_{\overline{\text{MS}}} = 338 \text{ MeV}$ , at different loop orders.
- **Strong dependence of  $\Lambda_{\overline{\text{MS}}}$  on  $\tau_F$**  in conversion, below  $\Lambda_{\overline{\text{MS}}} = 338 \text{ MeV}$ :

$$\Lambda_{\overline{\text{MS}}}^{N_f=3} = 311.0_{-0.7}^{+0.7} {}_{-4.8}^{+4.8} {}_{-11.7}^{+34.0} \text{ MeV}, \quad \alpha_{\overline{\text{MS}}}^{(N_f=5)}(M_Z) = 0.1162_{-0.0009}^{+0.0023}.$$

- Stat. error via bootstrap; symmetrized **cont. error** (leaving out  $\beta = 8.0$ ).
- **Truncation error estimate** by including  $\alpha_{\overline{\text{MS}}}^3$  with coefficient  $k_3 = \pm 2k_2$ .

## Summary

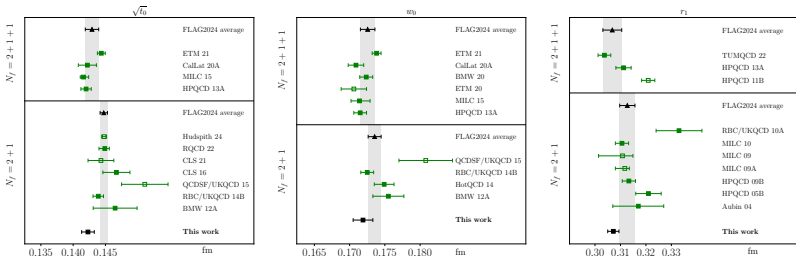
	$\sqrt{t_0}$ [fm]	$w_0$ [fm]	$r_1$ [fm]
$f_{\eta_s}$	0.14239(65)(94)	0.17139(80)(113)	0.3062(23)
$f_K$	0.14133(57)(82)	0.17012(74)(98)	0.3065(22)
$h_b - 1S$	0.1453(17)(15)	0.1752(21)(18)	0.3105(18)(31)
$\chi_b - 1S$	0.1441(17)(14)	0.1739(21)(17)	0.3104(18)(31)
$2S - 1S$	0.1477(40)(15)	0.1783(49)(18)	0.3119(76)(31)
wgt. avg.	0.14229 (98)	0.17190 (140)	0.3072 (22)



- We obtain gradient flow and potential scales in  $(2+1)$ -flavor QCD.
- Consistency between  $(2+1)$ - or  $(2+1+1)$ -flavor QCD: decoupling!

## Summary

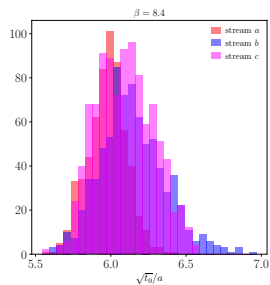
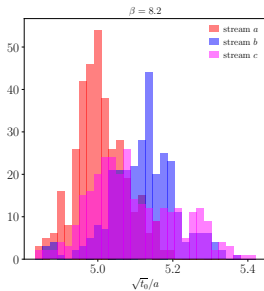
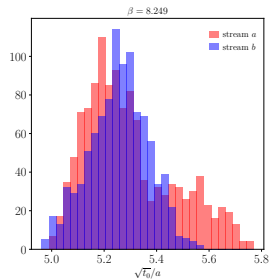
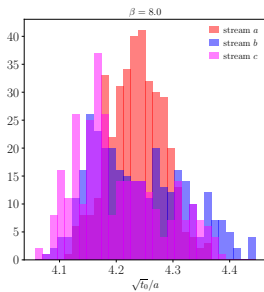
	$\sqrt{t_0}$ [fm]	$w_0$ [fm]	$r_1$ [fm]
$f_{\eta_s}$	0.14239(65)(94)	0.17139(80)(113)	0.3062(23)
$f_K$	0.14133(57)(82)	0.17012(74)(98)	0.3065(22)
$h_b - 1S$	0.1453(17)(15)	0.1752(21)(18)	0.3105(18)(31)
$\chi_b - 1S$	0.1441(17)(14)	0.1739(21)(17)	0.3104(18)(31)
$2S - 1S$	0.1477(40)(15)	0.1783(49)(18)	0.3119(76)(31)
wgt. avg.	0.14229 (98)	0.17190 (140)	0.3072 (22)



- We obtain gradient flow and potential scales in  $(2+1)$ -flavor QCD.
- Consistency between  $(2+1)$ - or  $(2+1+1)$ -flavor QCD: decoupling!

**Thank you for your attention!**



Effects of topology on  $\frac{\sqrt{t_0}}{a}$ 

Effects of topology on  $\frac{\sqrt{t_0}}{a}$ 